

# POLAR DESIGN AND MEASUREMENT TECHNIQUES FOR ELECTROMAGNETIC BANDGAP STRUCTURES

*C. B. Mulenga, A. Chauraya, J. A. Flint, J. C. Vardaxoglou*

Department of Electronic and Electrical Engineering, Loughborough University,  
Loughborough, Leicestershire, LE11 3TU, UK.  
c.b.mulenga@lboro.ac.uk  
j.a.flint@lboro.ac.uk

## Abstract

The purpose of this paper is two fold: first we propose a design technique for electromagnetic bandgap structures based on polar curves and mapping functions. The key advantage of this concept is that it allows increased capacitance without increasing element dimensions or thickness making it possible to increase or decrease the surface impedance on a per cell unit basis. Secondly, we report on a repeatable measurement technique for characterising the bandgap properties of EBG structures using an air spaced microstrip line. The device constructed is simple, economical, robust and capable of quantifying the properties of a wide range of EBG materials. In addition, the measurement technique is particularly applicable to fabric based EBG materials where measurements are especially challenging.

## 1 Introduction

Numerous kinds of EBG structures have been proposed and applied to antennas and microwave circuits. EBG structures are inherently periodic dielectric and/or metallic structures used to control and manipulate the flow of electromagnetic waves. EBG structures essentially behave as L-C resonant circuits with a pass-band and stop-band operation. Antennas operating within the stop-band region have their reflected waves in-phase with the incident waves. This occurrence together with the fact that surface waves are also suppressed, has led to the creation of low profile antennas, reduction of mutual coupling in antenna arrays and a host of other applications. EBG structures are often implemented using the mushroom geometry proposed by Sievenpiper [1] utilizing the plain square as the fundamental element of design. The mushroom structure (Fig. 1) consists of a ground plane, dielectric substrate, vias and an FSS layer made up of periodically loaded patches. Several configurations have been proposed in the literature to realize the FSS layer.

Parker *et al.* in [2] suggests that the size of the unit cell should be reduced if FSS designs are to be applied to curved surfaces. Reduced cell sizes eliminate element distortions that can occur when FSS designs are overlaid on surfaces with intricate curvatures. Tse *et al.* [3] proposed the use of convoluted and interleaved dipole elements to reduce bandgap frequency for fixed periodicity. The use of convoluted FSS was taken further to include Hilbert space filling curves [4]. This approach to reducing unit cell dimensions, increases the electrical length of the element by over 5 times leading to substantial reductions in resonant frequencies.

EBG structures are characterised not only by their resonant frequency but also their bandwidth. The bandwidth of an EBG surface is quantified by the breadth of its bandgap. Various measurement methods can be found in the literature for characterising the bandgap of these structures. Methods that use coaxial monopole probes, current loop probes, and flared parallel-plate waveguides (first proposed in [1]) which form the baseline for TE and TM surface wave measurements are a popular means of characterising the bandgap property. Other researchers have preferred to illustrate the superiority of their designs by directly applying the designed structures to a specific application for example low profile antennas [5]. The leading challenge in all these measurement methods is the added requirement to tailor them to suit a particular application or frequency range on which they are heavily reliant.

Therefore, in this paper we propose as follows: first, mathematical expressions for the design of EBG structures using polar curves and mapping functions and an application of this concept to high impedance surfaces. The aim is to demonstrate the potential of polar curves and mapping functions in the design of electromagnetic band gap structures including those on non-planar surfaces and with non-uniform unit cell. Secondly, the use of an air spaced-microstrip line based device for the bandgap characterisation of EBG structures is introduced. In this technique, the microstrip line can be described as exhibiting quasi-plane wave excitation. The key advantage of this method is the ability to increase the bandgap accurately.

## 2 Design

### 2.1 EBG

The geometry of the unit cell of the Polar-EBG structure is based on a square patch (Fig. 1) connected to the dielectric backed ground by conducting via. The patch width is equal to the periodicity of a conventional mushroom structure making the two structures footprint equal. The square patch is converted to a polar form by means of the equation below.

$$F(\theta, k) \approx T \times \left[ \frac{w[\theta] - \sin^{-1}(\cos(k\theta))}{\pi} \right] \quad (1)$$

where  $T$  is width of the mushroom element,  $w[\theta]$  is a mapping function,  $k$  is the curve order number and  $\theta$  is an angle that varies between  $0 \leq \theta \leq (1.5\pi + 0.5\pi/k)$ . Subsequently, interleaved tessellating slots of a fixed width which optimize the inter element coupling for each element are cut from the mushroom element (Fig. 1a). In order to take advantage of the square lattice, a mapping function (Fig. 1b) that provides a warping transformation stretches the circular spiral pattern so that it fills the whole cell. By means of this approach the longest length slot is obtained providing a means of increasing the resonant current path within the unit cell necessary for maximizing the fringing capacitance. The length of the slot governed by the curve order,  $k$  (Fig. 1c) transforms the slot length (number of turns of the spiral) which in turn adjusts the surface impedance of the unit cell element. Thus, variation of the spiral windings (slot length) results in the tuning of the frequency bandgap position without any need for alterations in the unit cell dimensions.

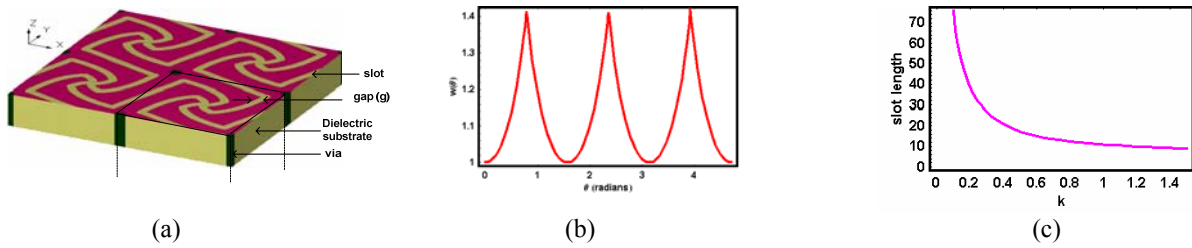


Fig. 1: (a) Schematic of 2×2 Polar-EBG (b) Mapping function (c) Variation of slot length with curve order,  $k$

### 2.2 Measurement Apparatus

The apparatus constructed for measuring the device (Fig. 2a) consists of a dielectric backed tapered microstrip line supported by screws at a height of 5 mm above the ground plane. The ends of the microstrip line are connected to a coax port. Fig. 2(b) illustrates the topology of the microstrip line fabricated on FR4 substrate while Fig. 2(c) shows the measurement setup incorporating the surface under test (SUT). In order to match the microstrip line to the coaxial port, various tapering configurations were investigated from which it was determined that the triangular taper provided the optimal match. Further optimization of the structure was undertaken to determine the optimal values of  $p$  and  $d$  whereby reflection is minimized and transmission is maximized. Fig. 3 shows the return loss and transmission coefficient results for various values of  $p$  and  $d$  simulated in the TLM based commercial solver MicroStripes v7.5. The optimal values found for the triangular tapered microstrip line were  $p = 180$  mm and  $d = 10$  mm with a microstrip width  $W = 23$  mm and substrate spacing  $h = 5$  mm. The ground plane dimensions adopted herein are  $200 \times 100$  mm.

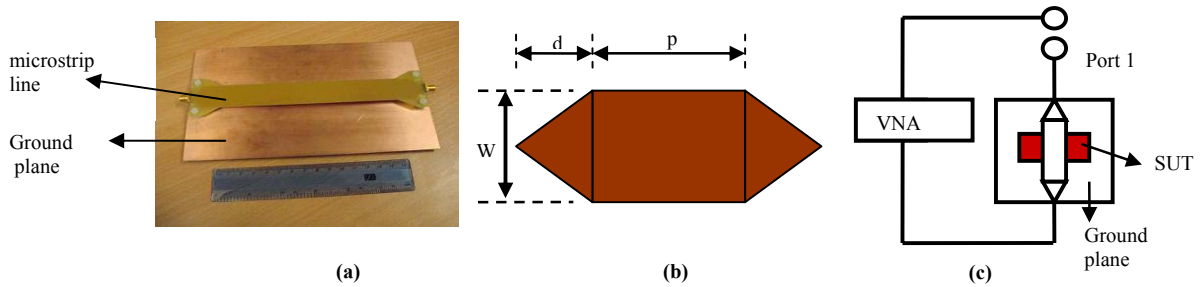
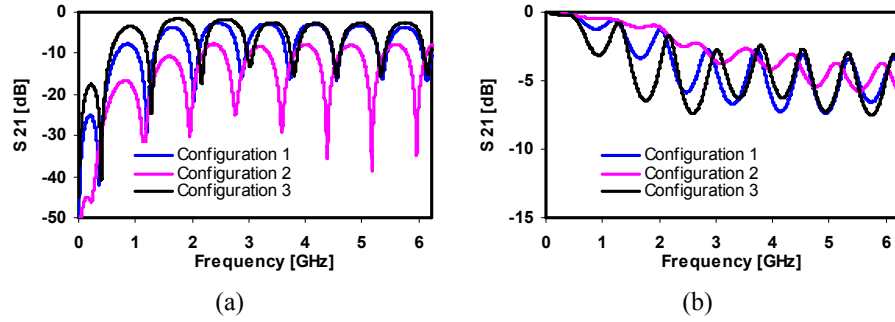


Fig. 2: (a) Geometry of an air spaced microstrip line (b) Top view of tapered microstrip line (c) Schematic of measurement setup



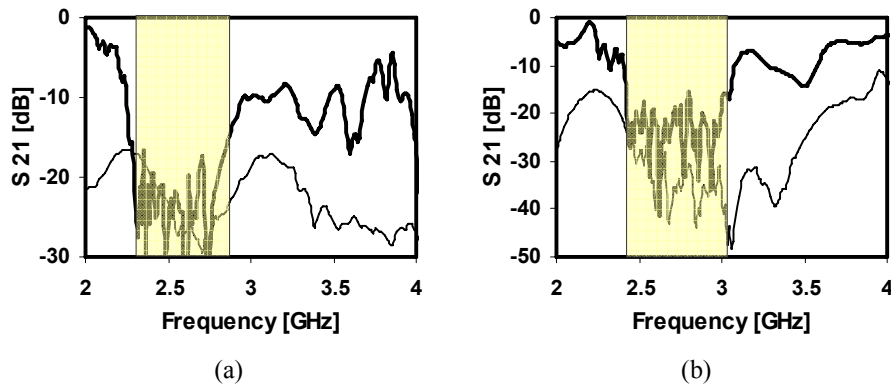
**Fig. 3: (a) Return Loss (b) Transmission Coefficient (i) Configuration 1:  $d = 46$  mm ,  $p = 108$  mm (ii) Configuration 2:  $d = 10$  mm,  $p = 180$  mm (iii) Configuration 3:  $d = 25$  mm,  $p = 150$  mm**

### 3 Results

To verify the surface wave properties of the proposed Polar-EBG, three Polar-EBG surfaces together with the conventional mushroom structure having the same periodic spacing were fabricated on a Taconic TLE-95 substrate of height 3.18 mm and dielectric constant  $\epsilon_r = 2.95$ . The periodic spacing was chosen as 7.5 mm, the gaps were varied between 0.25 mm, 0.5 mm and 0.75 mm, while the curve order  $k = 0.5$  was maintained throughout. The surface under test was constructed as a  $12 \times 12$  array. Both TE and TM surface wave measurements were carried out using a pair of monopole coax probes with the radiating element of diameter 0.92 mm and height 27.91 mm corresponding to  $0.25\lambda$  at 2.7 GHz. Prior to measuring the surface the characteristics of the microstrip line were measured using the VNA calibrated to two coaxial ports. These outputs are shown in Fig. 3 were used to optimise the line design. Once the best configuration was found the apparatus was attached to port 1 on the analyser and the instrument recalibrated so that the reference plane at port 1 was the apparatus output (Fig. 2c). Thus the instrument calibration effectively removes the imperfections in the transmission line. The S<sub>21</sub> is a flat line at 0 dB when the measurement setup is calibrated. It can be seen in Fig. 4 that the results obtained are superior to those obtained using the more commonly-used probe technique for determining the bandgap. The bandgap region shown on the graphs is compared to numerical values derived using equations determined in [1] for the resonant frequency ( $\omega_0$ ) and bandwidth ( $B.W.$ ).

$$\omega_0 = \frac{1}{\sqrt{LC}} \quad \text{and} \quad B.W. = \frac{\Delta\omega}{\omega_0} = \frac{1}{\eta} \sqrt{\frac{L}{C}} \quad (2)$$

Overall, the measurement results obtained using the air-spaced microstrip line are in excellent agreement with the coax monopole results. The difference in bandgap width between the two measurements can be attributed to the presence of multiple interference which results from occurrences of multiple signal paths when coax probes are used for measurements. In addition to this, the gap widths in the fabricated Polar-EBG structures varied by  $\pm 3\%$  introducing further variations in the bandgap widths. As no post-processing of the measurement data is required, the air-suspended microstrip line technique makes the determination of the bandgap of EBG structures very straight forward.



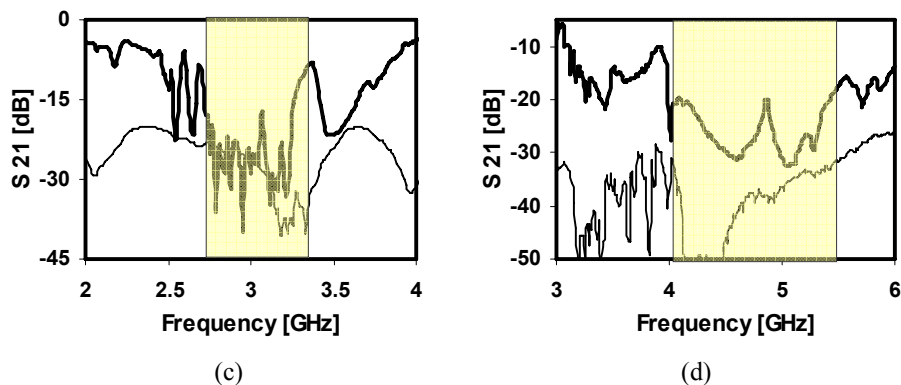


**Fig. 4: Comparison of bandgap regions based on measurement results using air spaced microstrip line (thick Line) and a pair of coax monopoles (thin line) (a) gap width 0.25 mm (b) gap width 0.5 mm (c) gap width 0.75 mm (d) mushroom structure. The coloured region shows the bandgap as numerically determined using equations proposed in [1]**

#### 4 Conclusion

The EBG structure designed using polar curves and mapping functions has the same basic operation as the conventional mushroom structure as demonstrated by the presence of a bandgap. The surface wave suppression capabilities were investigated experimentally using monopole probes and an air spaced microstrip technique. It is revealed that the Polar-EBG exhibits reduced resonant frequency when compared to a mushroom EBG of equal dimensions. Although the concept of designing EBG structures using polar curves and mapping functions has been shown to have potential, it is clear that the bandwidth of operation is reduced and if this is a critical consideration other changes to the geometry, such as surface thickness may be taken into consideration.

#### Acknowledgements

The authors gratefully acknowledge Taconic who provided the laminate samples for the designs and Flomerics Group PLC who supplied the modelling software Microstripes.

#### References

- [1] D. Sievenpiper, L. Zhang, E. Yablonovitch and R. Broas, "High-impedance electromagnetic surfaces with forbidden bands at radio and microwave frequencies," *Proc SPIE Int Soc Opt Eng*, **3795**, 1999, pp. 154-165.
- [2] E. A. Parker, A. N. A. El Sheikh and A. C. d. Lima, "Convolutd frequency-selective array elements derived from linear and crossed dipoles," *Microwaves, Antennas and Propagation IEE Proceedings*, **140**, 1993, pp. 378-380.
- [3] S. Tse, B. S. Izquierdo, J. C. Batchelor and R. J. Langley, "Convolutd elements for electromagnetic band gap structures," in *IEEE International Symposium on Antennas and Propagation*, Monterey, California, USA, 2004, pp. 819-822.
- [4] G. S. A. Shaker and S. Safavi-Naeini, "Reduced size Electromagnetic Band Gap (EBG) structures for antenna applications," *Canadian Conference on Electrical and Computer Engineering*, **2005**, 2005, pp. 1198-1201.
- [5] J. R. Sohn, H. Tae, J. Lee and J. Lee, "Comparative analysis of four types of high-impedance surfaces for low profile antenna applications," *IEEE AP-S International Symposium (Digest) on Antennas and Propagation Society*, **1A**, 2005, pp. 758-761.